

# Determination of Complex Residual Error Parameters of a Calibrated Vector Network Analyzer

Gerd Wübbeler\*, Clemens Elster\*, Thomas Reichel<sup>x</sup>, and Rolf Judaschke<sup>‡</sup>

\* Physikalisch-Technische Bundesanstalt, Abbestr. 2-12, D-10587 Berlin, Germany

Email: gerd.wuebbeler@ptb.de, clemens.elster@ptb.de

<sup>x</sup> Rohde & Schwarz GmbH & Co. KG, Mühldorfstr. 15, D-81671 München, Germany

Email: thomas.reichel@rsd.rohde-schwarz.com

<sup>‡</sup> Physikalisch-Technische Bundesanstalt, Bundesallee 100, D-38116 Braunschweig, Germany

Email: rolf.judaschke@ptb.de

**Abstract**—A novel technique for the determination of the residual directivity and the residual source match of a calibrated one-port vector network analyzer is investigated. The method corresponds to the “ripple extraction” schemes and is based on a single reflection measurement employing a high precision airline terminated by a short. The complex-valued residual system errors are not directly measured, but will be extracted over the entire measured frequency range by a sophisticated data analyzing scheme utilizing, among other things, bandpass filtering and linear prediction. By modeling the utilized short, also the residual reflection tracking can be estimated. Thus, in comparison with a standard SOL calibration (performed with sliding load), a VNA accuracy enhancement can be achieved by second-order error correction.

**Index Terms**—vector network analyzer calibration, residual error parameter, linear prediction.

## I. INTRODUCTION

The vector network analyzer measurement uncertainty depends on the calibration method applied, the modeling accuracy of the calibration standards, and the system parameters like stability, noise, and connector repeatability. Even though the resulting measurement uncertainty could theoretically be derived from the above mentioned factors, estimations of the residual error model parameters are obtained experimentally and utilized for uncertainty calculation and furthermore, verification of the VNA calibration.

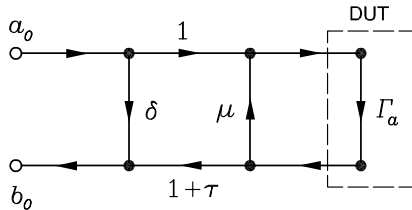


Fig. 1. One-port error model.

Based on the commonly applied one-port error model

(Fig. 1), the measured reflection coefficient  $\Gamma_m$  is related to the actual DUT value  $\Gamma_a$  by

$$\Gamma_m = \frac{b_0}{a_0} = \delta + (1 + \tau) \frac{\Gamma_a}{1 - \mu \Gamma_a} \quad (1)$$

where  $\delta$  denotes the residual directivity,  $\tau$  the residual reflection tracking, and  $\mu$  the residual source match of a calibrated VNA. For simplification, (1) can be approximated by

$$\Gamma_m \approx \delta + (1 + \tau) \Gamma_a + \mu \Gamma_a^2 \quad (2)$$

To determine  $|\delta|$  and  $|\mu|$ , respectively, the input reflection coefficient of a precision airline terminated by a mismatch ( $|\delta| < |\Gamma_L| < 0.1$ ) and a short, respectively, is measured, followed by a ripple extraction scheme to estimate the magnitude of both parameters [1]. This method has been refined in [2] for the determination of  $\delta$  in both magnitude and phase.

In contrast to the established methods, the novel technique [3], [4] to be investigated in this paper, precisely determines both the residual directivity  $\delta$  and the source match  $\mu$  in magnitude and phase by post-processing the data of a *single* input reflection coefficient measurement of a short-circuited precision airline. Furthermore, by modeling the utilized short, the residual complex reflection tracking can be estimated.

## II. COMPLEX RESIDUAL ERROR PARAMETER DETERMINATION

The novel technique is based on the separation of the time-delayed portions composing the input reflection coefficient of a short-circuited airline [3], [4]. The separation is performed in time-domain by sequences of down-conversion, low-pass filtering, and up-conversion of the measured reflection coefficient  $\Gamma_m(f)$ .

Starting from the signal flow shown in Fig. 2 and assuming a high precision airline ( $S_{11} = S_{22} \approx 0$ ), we get

$$\Gamma_a \approx -e^{-2\gamma l} \quad (3)$$

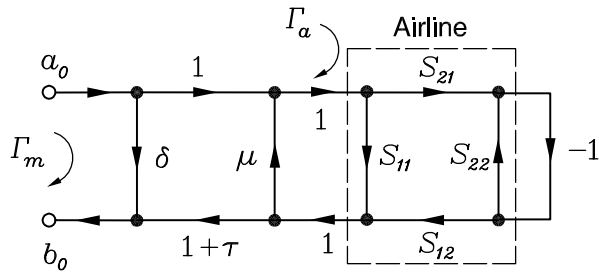


Fig. 2. One-port signal flow graph measuring a short-circuited airline.

and by using (2)

$$\Gamma_m \approx \underbrace{\delta}_A - \underbrace{(1+\tau)e^{-2\gamma l}}_B + \underbrace{\mu(1+\tau)e^{-4\gamma l}}_C, \quad (4)$$

where  $\gamma = \alpha + j\beta$  denotes the propagation constant. Figure 3 shows a typical reflection coefficient  $|\Gamma_m|$  of a short-circuited airline (length 150 mm), measured by a SOL-calibrated VNA (using a broadband load).

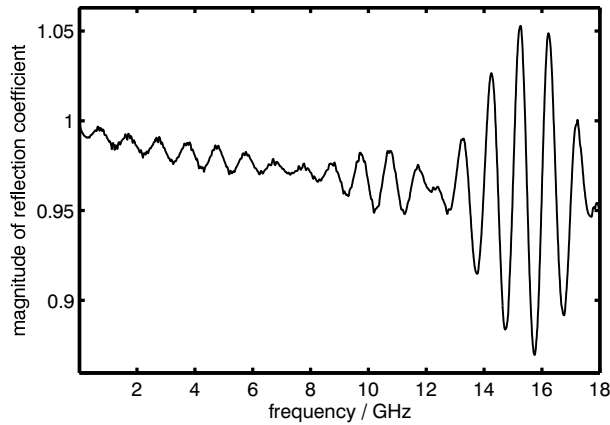


Fig. 3. Measured magnitude of input reflection coefficient of a short-circuited airline.

As indicated in (4), the reflection coefficient  $\Gamma_m$  consists of the residual directivity (A), a short-circuit term (B), and a source-match term (C), chronologically separated of each other in time-domain. This is illustrated in Fig. 4, where a Fourier transformation has been applied to the measured 1601 data points shown in Fig. 3.

The three terms (A), (B) and (C) in (4) are separated utilizing the following procedure [3], [4]: First, the dominant short-circuit term (B) is determined. For this purpose, down-conversion is applied to  $\Gamma_m$  yielding

$$\begin{aligned} \tilde{\Gamma}_m &= \frac{\Gamma_m}{e^{-2\gamma l}} \\ &= \delta e^{2\gamma l} - (1+\tau) + \mu(1+\tau)e^{-2\gamma l}, \end{aligned} \quad (5)$$

where  $l$  is estimated as the sum of the length of the airline and the offset length of the utilized short. The propagation

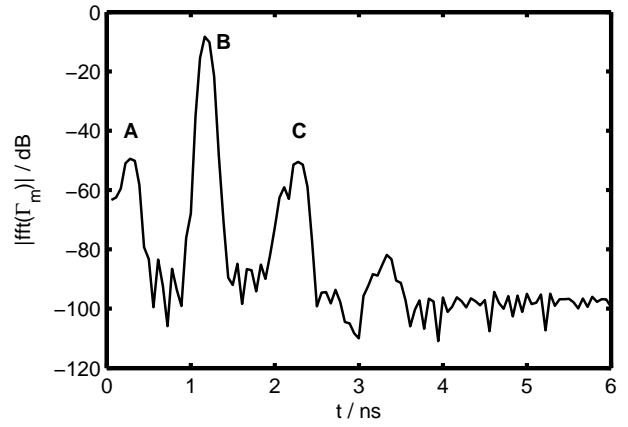


Fig. 4. Time-domain response of  $\Gamma_m$  as shown in Fig. 3.

constant  $\gamma$  is approximated as

$$\gamma \approx j\frac{\omega}{c}, \quad (6)$$

where  $\omega$  denotes the angular frequency and  $c$  the vacuum speed of light. Since  $\delta$ ,  $\mu$  and  $\tau$  are slowly varying functions of  $\omega$  as compared to  $e^{-2\gamma l}$ , the terms  $\delta e^{2\gamma l}$  and  $\mu(1+\tau)e^{-2\gamma l}$  in (5) can be removed by appropriate low-pass filtering. Yet, the output of this filtering should not be used as an estimate of  $(1+\tau)$ , since the approximation of  $\gamma$  is not precise enough for this purpose. Rather by multiplication of the filter output with  $e^{-2\gamma l}$  (i.e. by up-conversion) an estimate of the term (B) is obtained.

The low-pass filtering is performed in time-domain (after Fourier transformation) by applying a hard rectangular filter followed by back-transformation into frequency domain. Due to the finite measured frequency range and the usually non-periodical behavior of the reflection coefficient, the hard rectangular filter induces artifacts on both ends of the measured frequency range. In order to suppress these artifacts, data extrapolation via linear prediction [5] is applied in frequency domain. For this, the coefficients  $a_k$  of an autoregressive (AR) model

$$y_n = \sum_{k=1}^M a_k y_{n-k} + \epsilon_n, \quad (7)$$

of order  $M$  (with  $\epsilon_n$  representing white noise) are estimated from  $\tilde{\Gamma}_m$  in frequency domain using the Burg algorithm [6]. In (7),  $y_n$  denotes either real or imaginary part of the reflection coefficient  $\tilde{\Gamma}_m$  at frequency  $\omega_n$ . After having estimated the model parameters  $a_k$ , (7) is applied to extrapolate the data at both ends of the measured frequency range. Estimation of AR-coefficients  $a_k$  and extrapolation is done independently for real and imaginary part of the measured data. In Fig. 5, the extrapolation is illustrated using the reflection data from Fig. 3 after down-

conversion. For additional artifact reduction, mirroring is applied to the extrapolated data (not shown in Fig. 5).

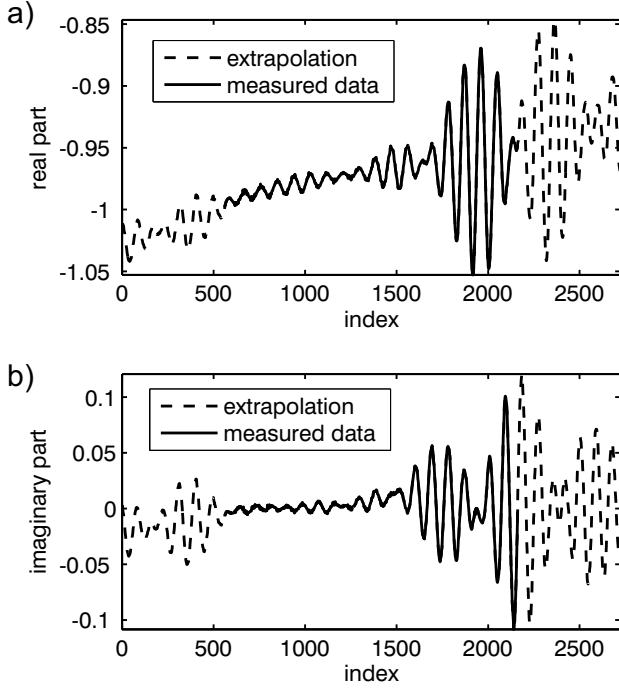


Fig. 5. Extrapolation by linear prediction applied to the down-converted reflection coefficient  $\tilde{\Gamma}_m$ : real part a) and imaginary part b), measurement (—), extrapolation (---).

Having determined the dominant part ( $B$ ) in (4), next, the component ( $A$ ), i.e. the residual directivity  $\delta$  is estimated by low-pass filtering of

$$\Gamma_{AC} = \Gamma_m - B \approx A + C = \delta + \mu(1 + \tau)e^{-4\gamma l}. \quad (8)$$

Again, the same extrapolation and hard rectangular filtering scheme is applied as described above. For estimation of the third component ( $C$ ) in (4),

$$\tilde{\Gamma}_{AC} = \frac{\Gamma_{AC}}{B^2} \approx \frac{A}{B^2} + \frac{C}{B^2} \approx \frac{\delta}{(1 + \tau)^2} e^{4\gamma l} + \frac{\mu}{1 + \tau} \quad (9)$$

is calculated where ( $B$ ) denotes the above obtained estimate. Application of the extrapolation and low-pass filtering scheme to  $\tilde{\Gamma}_{AC}$  then gives

$$\frac{C}{B^2} = \frac{\mu}{1 + \tau}. \quad (10)$$

Note, that the residual reflection tracking  $\tau$  should not directly be estimated from the component ( $B$ ) since the propagation coefficient  $\gamma$  is not known with sufficient accuracy. Alternatively, consistency between the model  $\Gamma_{sc}$  of the used short and its corrected reflection coefficient is utilized:

$$\Gamma_{sc} = \delta + (1 + \tau) \frac{\Gamma_{sc}}{1 - \mu \Gamma_{sc}}. \quad (11)$$

The model  $\Gamma_{sc}$  of the used short is calculated from its offset length and its offset loss, according to the typical

calibration kit standard definition. From (11), the residual reflection tracking is estimated according to

$$\tau = -\frac{\frac{A}{\Gamma_{sc}} + \frac{C}{B^2}(\Gamma_{sc} - A)}{1 + \frac{C}{B^2}(\Gamma_{sc} - A)}, \quad (12)$$

where  $A$  denotes the obtained value of  $\delta$  and  $C/B^2$  the estimate according to (10). Finally, the residual source match is obtained from (10) as

$$\mu = \frac{C}{B^2}(1 + \tau). \quad (13)$$

The performance of the proposed scheme mainly depends on the choice of three parameters, namely the bandwidth of the low-pass filter, the degree of extrapolation and the order  $M$  of the autoregressive model. In order to choose appropriate values for these parameters, simulated data were constructed and analyzed for various settings of these parameters.

### III. RESULTS

The method has been applied to data sets obtained from airlines of different length measured shortly one after another using the same VNA calibration.

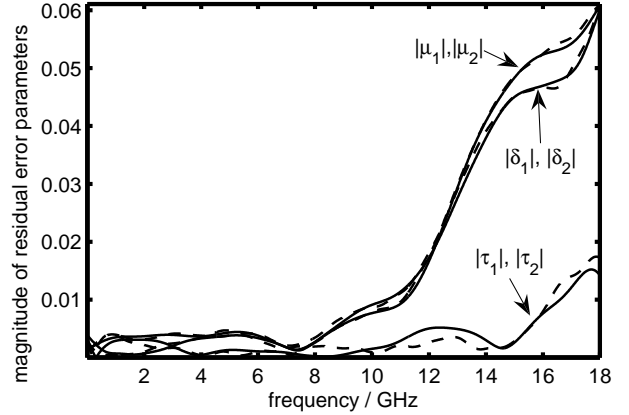


Fig. 6. Comparison of extracted error parameters: magnitude of  $\delta$ ,  $\mu$ , and  $\tau$ , obtained from measured data: 300 mm airline 1 (—), 150 mm airline 2 (---).

A comparison of the extracted error parameters shows close agreement in both magnitude (Fig. 6) and phase (Fig. 7) of the residual error parameters. It should be emphasized that for both data sets identical method parameters were used for the extraction of the residual error parameters. The observed consistency underlines the robustness of the proposed technique.

Using the complex error parameters, the input reflection  $\Gamma_a$  of the 150 mm airline has been calculated according to (1) and plotted in Fig. 8 (dashed line). Obviously, the oscillations vanish, and the return loss is in agreement with theoretical results taking into account airline losses due to skin effect. As shown in [4], the residual error parameters

can also be used to apply a second-order calibration of the VNA in order to achieve a higher measurement accuracy.

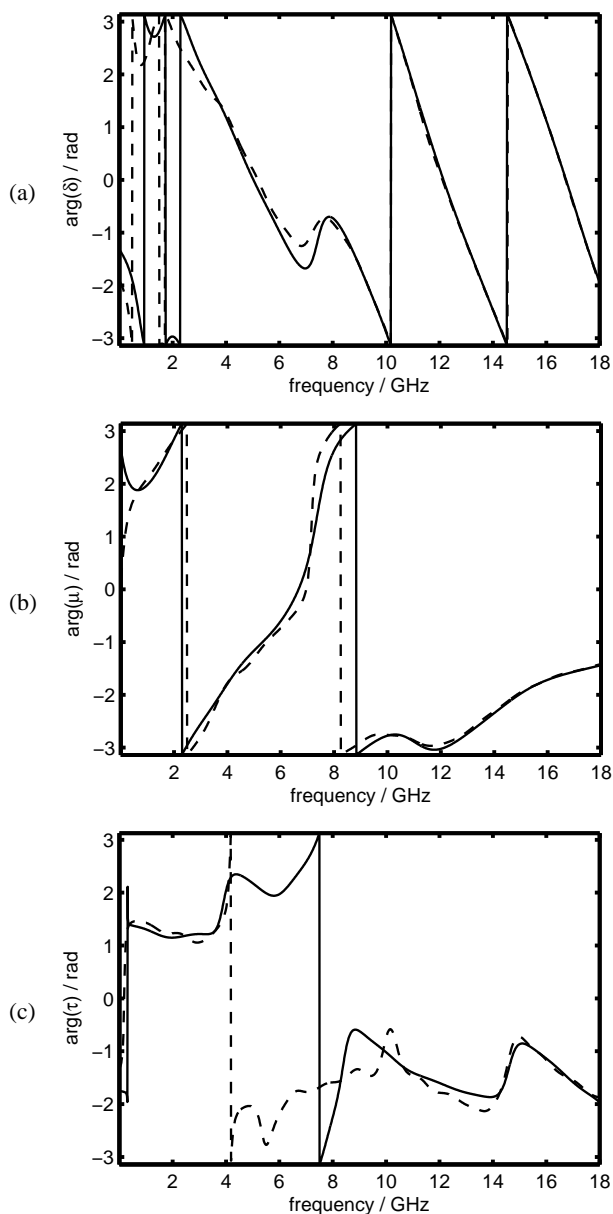


Fig. 7. Comparison of extracted error parameters: phase of  $\delta$  (a),  $\mu$  (b), and  $\tau$  (c), obtained from measured data: 150 mm airline 1 (—), 300 mm airline 2 (---).

#### IV. CONCLUSION

In this work it is shown that the reflective residual error parameters of a calibrated VNA can be determined from a single reflection measurement with the help of an appropriate signal processing technique. With the proposed method, the complex-valued residual error parameters can be determined in a robust way over the entire measured frequency range.

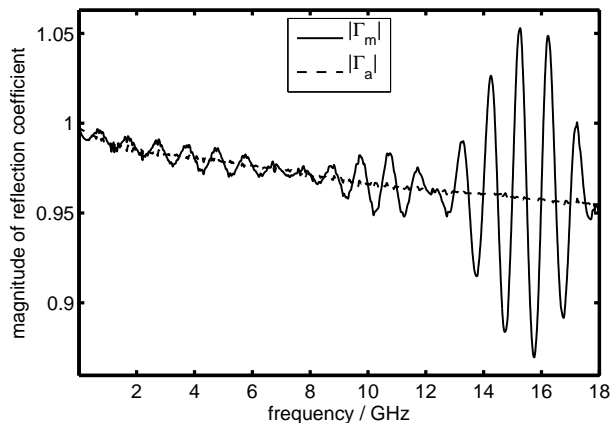


Fig. 8. Measured magnitude of input reflection coefficient of a short-circuited 150 mm airline (—), calculated reflection coefficient using extracted residual parameters as shown in Fig. 6 and Fig. 7. (---).

#### REFERENCES

- [1] EA-10/12, "Guidelines for the Evaluation of Vector Network Analysers (VNA)", EA - European co-operation for Accreditation, May 2000.
- [2] P. Persson, "An Algorithm for the Evaluation of the Residual Directivity "ripple" trace", ANAMET Report 034, May 2002.
- [3] T. Reichel, H. Jäger, "Method for Measuring the Residual System Directivity and/or the Residual System Port Impedance Match of a System-calibrated Vector Network Analyser", European Patent No. EP 1 483 593 B1, 2006.
- [4] T. Reichel, "Ein neues, luftleitungsgestütztes Kalibrierverfahren für Netzwerkanalysatoren", in H. Bachmair (ed.), *Neue, innovative Kalibrierverfahren im Nieder- und Hochfrequenzbereich*, 218. PTB-Seminar, May 2006.
- [5] J. Makoul, "Linear Prediction: A Tutorial Review," *Proceedings of the IEEE*, vol. 63, no. 4, April 1975.
- [6] Matlab, The MathWorks, Inc.